

# Inter-Mobile-Device Distance Estimation using Network Localization Algorithms for Digital Contact Logging Applications

Lillian Clark<sup>a,\*</sup>, Alan Papalia<sup>b</sup>, Jônata Tyska Carvalho<sup>c</sup>, Luca Mastrostefano<sup>d</sup>, Bhaskar Krishnamachari<sup>a</sup>

<sup>a</sup>*Ming Hsieh Department of Electrical and Computer Engineering, University of Southern California, United States*

<sup>b</sup>*Computer Science and Artificial Intelligence Laboratory, Massachusetts Institute of Technology, United States*

<sup>c</sup>*Department of Informatics and Statistics (INE), Federal University of Santa Catarina, Brazil*

<sup>d</sup>*Covid Community Alert, United Kingdom*

---

## Abstract

Mobile applications are being developed for automated logging of contacts via Bluetooth to help scale up digital contact tracing efforts in the context of the ongoing COVID-19 pandemic. A useful component of such applications is inter-device distance estimation, which can be formulated as a network localization problem. We survey several approaches and evaluate the performance of each on real and simulated Bluetooth Low Energy (BLE) measurement datasets with respect to both distance estimate accuracy and the proximity detection problem. We investigate the effects of obstructions like pockets, differences between device models, and the environment (i.e. indoors or outdoors) on performance. We conclude that while direct estimation can provide the best proximity detection when Received Signal Strength Indicator (RSSI) measurements are available, network localization algorithms like Isomap, Local Linear Embedding, and the spring model outperform direct estimation in the presence of missing or very noisy measurements. The spring model consistently achieves the best distance estimation accuracy.

---

## 1. Introduction

Mobile apps for automated contact logging using Bluetooth are being developed by many organizations to help contain the ongoing COVID-19 pandemic [1, 2, 3]. While many of these apps only detect if two devices are in proximity, it is helpful to also estimate the distance between the devices more accurately in order to determine the risk of possible infection. Distance can be estimated via the received signal strength of a Bluetooth beacon [4]. As the distance increases, the signal received weakens. However, these signals are often susceptible to high levels of statistical fluctuations due to scattering, absorption and reflections in the environment, leading to high variance in the signal strength measurements and low confidence in the distance estimate. This uncertainty has led many in the community, including Sven Mattison who co-invented Bluetooth, to doubt the feasibility of contact logging apps which rely on “vanilla point-to-point Bluetooth links” [5].

To overcome this, we can make use of the fact that in populated areas there are typically more than two devices present. For example, on buses, in grocery store lines, and in public parks, connectivity can be modeled with a graph, as in Figure 1. Edges on the graph represent the presence of Received Signal Strength Indication (RSSI) measurements between two devices. Shorter edges, bolded for emphasis, represent stronger signals which are typically less noisy and lead to better estimates. While we may have an RSSI-based distance estimate between two devices, like those shown in red, our objective is to improve on this estimate by leveraging the other available RSSI measurements. We can also use available RSSI measurements to estimate the distance between two devices for which a measurement is unavailable. This is possible assuming

---

\*Corresponding author

*Email addresses:* lilliamc@usc.edu (Lillian Clark), apapalia@mit.edu (Alan Papalia), jonata.tyska@ufsc.br (Jônata Tyska Carvalho), luca.mastrostefano90@gmail.com (Luca Mastrostefano), bkrishna@usc.edu (Bhaskar Krishnamachari)

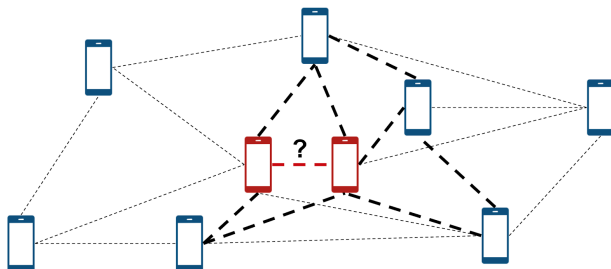


Figure 1: A network of available RSSI measurements, with more reliable measurements bolded. Our goal is to leverage all available measurements to get accurate distance measurements for any pair of devices, and improve accuracy for pairs with available measurements like the one shown in red.

a centralized architecture in which RSSI measurements are stored in a central server. While decentralized solutions have also been proposed, they pose various challenges [3]. The availability of a central server allows us to explore methods which improve distance estimation accuracy and will allow us to more confidently judge whether a device owner has been at risk.

The contribution of this work is a quantitative comparison of algorithms from the sensor network and learning communities which perform localization and can be used to estimate inter-device distances. In considering these methods, we focus on accuracy in distance estimation and proximity detection, i.e. detecting if two devices are within two meters. We evaluate each method on real and simulated data, with special attention to noisy and missing RSSI measurements, scalability, computational complexity, and common contact logging use cases. We qualitatively summarize our findings in Table 1 and present more detailed summaries in Section 6.2.

Table 1: Key Findings

Approach	Advantages	Disadvantages
Direct Estimation	Best proximity detection Lowest complexity	Not robust to missing RSSIs
Semidefinite Programming	Robust to missing RSSIs Best true positive rate Good distance estimation	Worst false positive rate
Spring Model	Robust to missing RSSIs Best distance estimation Good proximity detection	Some variance in performance Potential for divergent solutions
Non-linear manifold learning	Good proximity detection Good distance estimation	
Multidimensional Scaling (metric)		Not robust to missing RSSIs
Multidimensional Scaling (non-metric)	Good distance estimation	Poor proximity detection

This paper is organized into 7 sections. Section 2 presents relevant preliminaries including background, related work, and the RSSI-to-distance model used. Section 3 concisely formulates the problem. Section 4 presents the approaches evaluated in this work, with the appropriate details for reproducibility. Section 5 presents the results on data collected from real devices and Section 6 presents experiments on simulated

data to augment these results. We conclude with a summary and discussion of future work in Section 7. All relevant code for this paper can be found in [6].

## 2. Background and Related Work

In this work we are interested in determining the Euclidean distances between  $n$  devices or *nodes* based on measurements between them which are closely related to distance. To find the complete Euclidean distance matrix, we can first solve the problem of localizing  $n$  nodes in two-dimensional space. Note that since we are only interested in the relative locations, translations and rotations of the  $n$  points do not matter. The problem of mapping  $n$  points to two-dimensional space (or more generally, to a low-dimensional space) based on distances (often called *dissimilarities*) between them is well-studied and has a variety of applications.

In information visualization, the related problem of displaying complex data in 2D is commonly called graph realization, graph drawing, or graph embedding [7]. In cyberphysical systems, determining the physical locations of devices is typically called sensor network localization [8]. In machine learning, embedding datasets which exist in high-dimensional space into low-dimensional manifolds can be highly useful for things like semantic analysis, and is commonly called manifold learning [9].

Many approaches exist for solving the network localization problem. Multidimensional scaling (MDS) is a technique originally developed for use in mathematical psychology, and falls into two categories: metric or non-metric. In metric MDS, the input dissimilarity matrix is assumed to behave like distance, i.e. dissimilarities are a function of an underlying metric and is typically used whenever quantitative data is available [10, 11]. The goal of a metric MDS algorithm is to find a configuration of points in space such that the distances between two points are as close as possible to the dissimilarity data [12]. A non-metric MDS algorithm, by contrast, will try to preserve the order of the distances by finding a monotonic relationship between the distances in the two-dimensional space and the dissimilarities. Non-metric MDS is typically used when only qualitative data is available [10], although it is straightforward to derive ordinal data when quantitative data is available.

The goal of metric MDS can be written as an optimization over all possible configurations which minimizes a loss function. *Stress* is a commonly used loss function given by

$$\text{Stress}(\mathcal{X}) = \sqrt{\frac{\sum_{i=1}^n \sum_{j=1}^{i-1} (d_{ij} - \hat{d}_{ij})^2}{\sum_{i=1}^n \sum_{j=1}^{i-1} \hat{d}_{ij}^2}} \quad (1)$$

where  $d_{ij}$  is the dissimilarity between  $i$  and  $j$  and  $\hat{d}_{ij}$  is the distance between  $i$  and  $j$  in configuration  $\mathcal{X}$ . The classical approach, also called Principal Coordinates Analysis (PCoA), uses eigenvalue decomposition to find the optimal configuration  $\mathcal{X}$  [13]. An excellent description of classical MDS can be found in Appendix C of [8].

The disadvantage of classical MDS is that it requires dissimilarity measurements for *all* pairs of nodes, which are often not available in network localization problems. Work in distance matrix completion using graph distances or shortest paths can be used to first estimate a complete dissimilarity matrix, which allows the use of classical MDS [14, 15]. Another disadvantage of classical MDS is that it does not perform well when the dissimilarities are nonlinear. Isomap and Locally Linear Embedding (LLE) are two algorithms which extend classical MDS for nonlinear embeddings which use nearest neighbor search and are well-suited for manifold learning [12].

Other approaches to finding the optimal configuration  $\mathcal{X}$ , sometimes called stress majorization, take an iterative approach. A seminal work from Kruskal in the early 1960s describes an iterative steepest descent approach, wherein each point in an initially random configuration is adjusted slightly along the negative gradient of the stress with respect to that point's position. An extension of that work presents the Scaling by Majorizing a Complicated Function (SMACOF) algorithm, which is the basis for the multi-dimensional scaling function provided by the scikit-learn manifold library [16].

The previously mentioned approaches are centralized algorithms, however distributed variations exist. This class of algorithms starts with each node estimating its position, and then refining or relaxing this

estimate based on local information i.e. the dissimilarity and position estimates of its neighbors. Local neighborhood multilateration is presented in [17], where each node adjusts its position by using its neighbors as temporary beacons (reference points). An equivalent formulation to local multilateration is presented in [18] and is generally referred to as a spring model. In the graph formulation, edges between nodes are imagined as springs where the equilibrium length is the measured dissimilarity. Each node iteratively adjusts its position in the direction of its local spring force. While elegant, spring models are highly sensitive to initial starting positions, which can lead the algorithm to get stuck in local minima. One solution is to use unweighted graph distances to formulate a “fold-free” initial configuration [18]. Another approach is to relax the problem into a semidefinite program and apply the solution of the program as the initial configuration [19].

In the semidefinite program (SDP) approach to network localization, nonconvexities in the problem formulation are replaced with convex components in a way that attempts to closely model the nonconvex form of the original problem, and the resulting convex problem is then solved using common optimization machinery [20, 19]. Solutions to the SDP can be solved with approaches like the interior point algorithm, and these solutions can then be further refined by use of local, gradient-based optimization methods with the original problem formulation.

### 2.1. Related Work

Several surveys on localization exist in the sensor network community. The authors of [21] present an overview of measurement techniques, one-hop localization algorithms, and multi-hop localization algorithms including MDS and SDP, with a focus on the discussion of centralized versus distributed algorithms. Wang *et al.* [22] present a taxonomy of localization algorithms and performance analysis with respect to location accuracy, density and portion of the network with *a priori* known positions, computation cost and communication cost, while Chowdhury *et al.* [23] follow up with advances and recent trends. Our work, by contrast, focuses on different metrics including node-node distance estimation and proximity detection. In [24], simulation results are presented for three localization algorithms with a useful discussion of inter-node distance error. The algorithms presented depend on trilateration and the presence of three or more anchors (nodes with known initial positions), which is an assumption not made in this work. They conclude that no option performs the best under all conditions, motivating our investigation of network localization algorithms in this application-focused context.

The authors of [25] present a survey of distance metric learning, highlighting supervised methods and unsupervised methods like Isomap and LLE. Saeed *et al.* [26] present an overview of multidimensional scaling and its extensions, with specific attention to different loss functions. In [27], the authors present the results of linear and non-linear dimensionality reduction algorithms on real and simulated datasets. They are interested in the metrics of nearest-neighbor classification, continuity, and trustworthiness of the embedding, while this paper is specifically concerned with distance estimation accuracy and proximity detection. The authors of [28, 29] demonstrate the feasibility of using manifold learning algorithms for sensor network localization, bridging these related research thrusts and providing further motivation for this work.

Research in proximity detection for contact logging via RSSI measurements has been primarily concerned with feasibility and the relationship between RSSI and distance [4, 30], with a parallel research thrust in privacy-preservation [31, 32]. The contribution of this work is a survey of network localization algorithms and a comparative evaluation of their performance with respect to inter-mobile-device distance estimation and proximity detection in real and simulated data.

### 2.2. Pathloss Model

To estimate distance from RSSI, we use a radio propagation model which predicts the path loss a signal encounters over distance. In this work we use a simple path loss model with log-normal fading, a common noise model for RSSI signals. Formally,

$$P_r = P_T K \left( \frac{d}{d_0} \right)^\eta \psi \quad (2)$$

where  $P_r$  is the received power,  $P_T$  is the transmitted power,  $d$  is the distance between the devices,  $d_0$  is the reference distance,  $K$  is the gain at the reference distance (a number smaller than 1). The pathloss exponent  $\eta$  capture how quickly the signal falls off with distance, and is typically between 2 and 3. The noise is captured in the random variable  $\psi$ . Power is commonly measured on a decibel scale, where equation (2) is equivalently

$$P_{r_{dBm}} = P_{T_{dBm}} + K_{dB} - \eta 10 \log_{10} \frac{d}{d_0} + \psi_{dB} \quad (3)$$

where  $\psi_{dB}$  is now a zero-mean Gaussian random variable with variance  $\sigma_{dB}^2$ . It is often easier to assume the mean power received at a reference distance,  $P_{0_{dBm}}$  is known, and therefore

$$P_{r_{dBm}} = P_{0_{dBm}} - \eta 10 \log_{10} \frac{d}{d_0} + \psi_{dB} \quad (4)$$

Note that  $P_{r_{dBm}}$  is the measured RSSI, and it decreases linearly with log-distance. This means that the parameters  $P_{0_{dBm}}$ ,  $d_0$ , and  $\eta$  can be fitted using linear regression if a sample dataset is available. The standard deviation  $\sigma_{dB}$  can also be calculated from available data.

To calculate the distance estimate,  $d$ , if these parameters are known, we simply rearrange terms,

$$d = d_0 \left( 10^{-\frac{(P_{r_{dBm}} - P_{0_{dBm}})}{10\eta}} \right) \quad (5)$$

$$d_{min} = d_0 \left( 10^{-\frac{(P_{r_{dBm}} - P_{0_{dBm}} + 2\sigma_{dB})}{10\eta}} \right) \quad (6)$$

$$d_{max} = d_0 \left( 10^{-\frac{(P_{r_{dBm}} - P_{0_{dBm}} - 2\sigma_{dB})}{10\eta}} \right) \quad (7)$$

where distance is between  $d_{min}$  and  $d_{max}$  with 95.45% confidence.

### 3. Problem Formulation

The objective is to accurately estimate inter-device distances based on a matrix of available RSSI measurements. A possible matrix **RSSI** is shown below,

$$\begin{bmatrix} 0 & -65 & \emptyset & -68 & -66 \\ -66 & 0 & -72 & \emptyset & -73 \\ \emptyset & -73 & 0 & -68 & -71 \\ -68 & \emptyset & -68 & 0 & -59 \\ -66 & -71 & -71 & -58 & 0 \end{bmatrix}$$

where the measurement in the  $i^{th}$  row and  $j^{th}$  column represents the signal received at the  $i^{th}$  device and transmitted by the  $j^{th}$  device. The zeros along the diagonal represent the distance between a device and itself.  $\emptyset$  represents the absence of a measurement. Notice that for device pair  $i$  and  $j$ , the signal received by  $i$  may differ in strength from the signal received by  $j$ , such that the matrix is not symmetric.

From this matrix we seek to produce a symmetric matrix of distance estimates  $\hat{\mathbf{d}}$ , where  $\hat{d}_{ij}$  is the estimated distance between devices  $i$  and  $j$ . For example,

$$\begin{bmatrix} 0 & \hat{d}_{12} & \hat{d}_{13} & \hat{d}_{14} & \hat{d}_{15} \\ \hat{d}_{12} & 0 & \hat{d}_{23} & \hat{d}_{24} & \hat{d}_{25} \\ \hat{d}_{13} & \hat{d}_{23} & 0 & \hat{d}_{34} & \hat{d}_{35} \\ \hat{d}_{14} & \hat{d}_{24} & \hat{d}_{34} & 0 & \hat{d}_{45} \\ \hat{d}_{15} & \hat{d}_{25} & \hat{d}_{35} & \hat{d}_{45} & 0 \end{bmatrix}$$

In some cases we first find the configuration  $\mathcal{X} = \{x_1, x_2, \dots, x_n\}$  where  $x_1, \dots, x_n \in \mathcal{R}^2$ . This represents the location of each node in two-dimensional space, and we will refer to finding  $\mathcal{X}$  as the network localization problem. Given  $\mathcal{X}$ , we can calculate  $\hat{\mathbf{d}}$  since  $\hat{d}_{ij} = \|x_i - x_j\|$ .

## 4. Approaches to Estimating Inter-Device Distances

### 4.1. Direct Estimation

The simplest approach is to consider each RSSI measurement individually. In this case, for each entry in the **RSSI** matrix, we have one entry in the corresponding  $\hat{\mathbf{d}}$  matrix calculated with equation (5). This is the solution provided by direct estimation, but it is also the starting point for all other approaches. We refer to the set of node-node distance measurements available directly from the pathloss model as  $\mathcal{N}$ .

Note that direct estimation does not produce a symmetric distance matrix. We can choose to average the RSSI measurements prior to calculating distance, which we refer to as the pre-averaged approach, or average the calculated distance measurements, which we refer to as the post-averaged approach. Direct estimation also cannot produce distance estimates for missing RSSI for device pairs without RSSI measurements. We remedy this by assuming a threshold RSSI value (e.g.  $-95dB$ ) for missing measurements, which represents the noise floor of the receiver. This allows us to use the same evaluation metrics across the various approaches, as certain approaches require measurements between all nodes while others can use sparse RSSI matrices.

### 4.2. Semidefinite Programming

Distances can be estimated by performing network localization. To solve the network localization problem, we use the open source convex optimization libraries CVXPY [33, 34] and SCS [35, 36], which use the alternating direction method of multipliers to solve a previously obtained semidefinite program (SDP) [19]. This approach makes use of what are known as anchors and nodes. Anchors are sensors in which the location is known *a priori*. Nodes are sensors in which position is unknown, where these locations are the estimated variables of interest. Generally, an increased number of anchors leads to an improved final solution [37], however anchors are not required for our specific approach [19]. We present the generalized version of our SDP solution, with the understanding that in the case of inter-device distance estimation there are potentially no anchors. Numerical results suggest that in the case of no anchors, arbitrarily assigning a single node to be an anchor with an arbitrary, predefined location can improve solver stability and solution quality.

The approach we take looks to solve a problem of the form below, which is the form of Maximum Likelihood Estimation (MLE) measurements with additive Gaussian noise [19, 38].

$$\arg \min_{\mathcal{X}} \left\{ \begin{array}{l} \sum_{(i,j) \in \mathcal{N}} \frac{1}{\sigma_{ij}^2} \left| \|x_i - x_j\|^2 - d_{ij}^2 \right| \\ + \sum_{(i,j) \in \mathcal{M}} \frac{1}{\sigma_{ij}^2} \left| \|x_i - a_j\|^2 - d_{ij}^2 \right| \end{array} \right\} \quad (8)$$

Seen above,  $\mathcal{N}$  is the set of all available node-node distance measurements,  $\mathcal{M}$  is the set of all anchor-node distance measurements,  $\sigma_{ij}$  is the variance of measurement between sensors  $i$  and  $j$ ,  $x_i$  and  $x_j$  are variables representing the positions of nodes  $i$  and  $j$ ,  $a_j$  is a constant vector representing the known position of anchor  $j$ , and  $d_{ij}$  represents the distance measurement between the corresponding sensors  $i, j$ .

However, it is easily shown that the objective function displayed in equation (8) is non-convex, and as such we cannot guarantee the ability to optimally solve the problem with standard convex solvers. To remedy this, a convex relaxation can be made which replaces the non-convexities in a manner which attempts to preserve the general form of the problem. In the implementation chosen, a semidefinite relaxation is made which relaxes a non-convex quadratic constraint in the problem. For those interested in the particular details of the formulation, we direct you to [19].

It is notable that though reformulating the problem into this convex form allows for usage of convex programming and guarantees the ability to find the global minimum of the relaxed problem, it comes at a loss of accuracy in the cost function. As a result, though the optimal solution is often a good estimate for the network localization problem it is oftentimes not the global optimum. For this reason, the SDP solution is often used as a starting point for a local gradient-based solver of the original, non-convex problem.

### 4.3. Multidimensional Scaling

To find a solution to the network localization problem, we can use the MDS class provided by the Scikit-Learn Manifold library. This class implements the SMACOF iterative stress majorization algorithm, where at each step of the algorithm a Guttman transform of the current configuration is calculated [39]. A thorough description of the theory, implementation, and convergence results of SMACOF can be found in [40].

The MDS class can be configured to perform metric or non-metric MDS. Each takes as input a dissimilarity matrix, and our implementation provides the matrix given by the set of node-node distance measurements  $\mathcal{N}$ , and seeks to minimize

$$\text{Stress}_{\text{SMACOF}}(\mathcal{X}) = \sum_{(i,j) \in \mathcal{N}} \|x_i - x_j\| - g(d_{ij}) \quad (9)$$

where  $d_{ij}$  is the node-node distance measurement between  $i$  and  $j$  and  $g(d_{ij})$  is a linear function for metric MDS and monotonic function for non-metric MDS.

Note that the metric configuration requires a complete dissimilarity matrix i.e. the set  $\mathcal{N}$  must contain node-node distance measurements for all pairs. We again use the noise floor of the receiver when an RSSI measurement is not available. The non-metric implementation treats  $d_{ij} = 0$  for  $i \neq j$  as a missing entry rather than a distance of zero [12]. The solution  $\hat{\mathbf{d}}$  produced by non-metric MDS is then scaled by the average  $d_{ij}$  divided by the average  $\hat{d}_{ij}$  to produce a final network localization solution.

### 4.4. Spring Model

We present here a spring model (SM) that solves the network localization problem iteratively in a distributed manner in order to minimize the stress on each node,

$$\text{Stress}_{\text{SM}}(x_i) = F(x_i) = \sum_{j:(i,j) \in \mathcal{N}} f(x_i, x_j) \quad (10)$$

$$f(x_i, x_j) = \frac{\|x_i - x_j\| - d_{ij}}{d_{ij,max} - d_{ij,min}} \langle \frac{x_j - x_i}{\|x_i - x_j\|} \rangle \quad (11)$$

where we refer to stress as  $F(x_i)$  as it is the sum of forces applied to node  $i$  by each node  $j$ . These forces,  $f(x_i, x_j)$ , are analogous to the forces that would be applied if each node-node distance were a stretched or compressed spring. Note that these forces are vectors in the direction of  $\langle x_j - x_i \rangle$ , and the resulting stress is also a vector. In equation (11),  $d_{ij,max}$  and  $d_{ij,min}$  can be calculated from equations (6,7) and their difference provides a measure of uncertainty. Scaling the stress by this term allows distances with less uncertainty (typically shorter distances) to have a greater impact on the solution than distances with greater uncertainty.

Our spring model implementation is described in Algorithm 1, where  $n$  is the number of nodes,  $\mathcal{N}$  is the set of node-node distances,  $\epsilon$  is a parameter which defines convergence (we use 0.1), and  $\gamma$  is a coefficient applied to the force similar to a step size. To prevent the algorithm from diverging, we choose a step size of roughly  $\frac{1}{n}$ . We can optionally decrease  $\gamma$  over time for an adaptive step size, or update  $x_i \leftarrow x_i + \gamma(F^t + F^{t-1})$

to include momentum in the gradient descent.

---

**Algorithm 1:** Spring model for network localization

---

```

input :  $n, \mathcal{N}, \epsilon, \gamma$ 
output:  $\mathcal{X}$ 
initialize  $\mathcal{X}$  randomly in  $\mathcal{R}^2$ 
for iteration  $t$  do
  for node  $i$  do
     $F = 0$ 
    for node  $j$  do
      if  $(i, j) \in \mathcal{N}$  then
         $F \leftarrow F + f(x_i)$ 
      end
    end
     $x_i \leftarrow x_i + \gamma F$ 
  end
  stop if  $\|x_i^t - x_i^{t-1}\| \leq \epsilon \forall i \in \{1, \dots, n\}$ 
end

```

---

#### 4.5. Non-linear Manifold Learning

Along with the MDS class, the Scikit-Learn Manifold library provides several other classes for generalizing classical MDS to non-linear structures in data. In this work we implement Isomap to solve the network localization problem [41]. Isomap seeks to maintain geodesic distances between all points. Imagining the data as a graph where vertices are nodes and edges are available dissimilarity measures, the crux of Isomap is in estimating the distance between nodes which are not neighbors as the shortest path between them. Then Isomap performs eigenvalue decomposition to solve for node locations.

We also implement Local Linear Embedding (LLE), which preserves dissimilarities within local neighborhoods [42]. The crux of LLE is performing principal component analysis in each local neighborhood, then finding a globally optimal reconstruction of these partial solutions. Although the local embeddings assume linearity, the global solution can preserve non-linearities. As with non-metric MDS, our implementation of Isomap and LLE scales by the average  $d_{ij}$  divided by the average  $\hat{d}_{ij}$  to return a final solution.

## 5. Performance on Experimental Data

### 5.1. Bluetooth measurements for network of 11 devices

To evaluate the approaches presented in this work, we considered data collected from 11 devices used in an empty parking lot for which we have recorded locations and RSSI measurements from our previous work on radio frequency localization [43].

Figure 2 shows the spread of errors for each inter-device distance estimate. The absolute error is an intuitive measure of accuracy, but does not consider that large errors may be less significant when estimating large distances. For this reason we show the percent errors as well. From the plots we see that direct estimation approaches (RSS, pre-averaged, and post-averaged) have outliers, occasionally resulting in high errors. SDP, the spring model, and the spring model initialized with SDP all see low maximum percent errors. This is desirable because small variance leads to confident estimates.

Fitting probability density function (PDF) and cumulative density function (CDF) curves via gaussian kernel density estimation gives another way to interpret these errors, shown in Figure 3. For example, SDP is equally likely to result in an error of 5 meters as an error of 1 meter, with the most likely error of about 2 meters, which can lead to ambiguities. The spring model on the other hand, is unlikely to see errors above 4 meters, and most errors will be around 1 meter. The CDFs allow us to look for stochastic dominance, where the leftmost curve represents the approach which dominates the others. When considering the absolute error



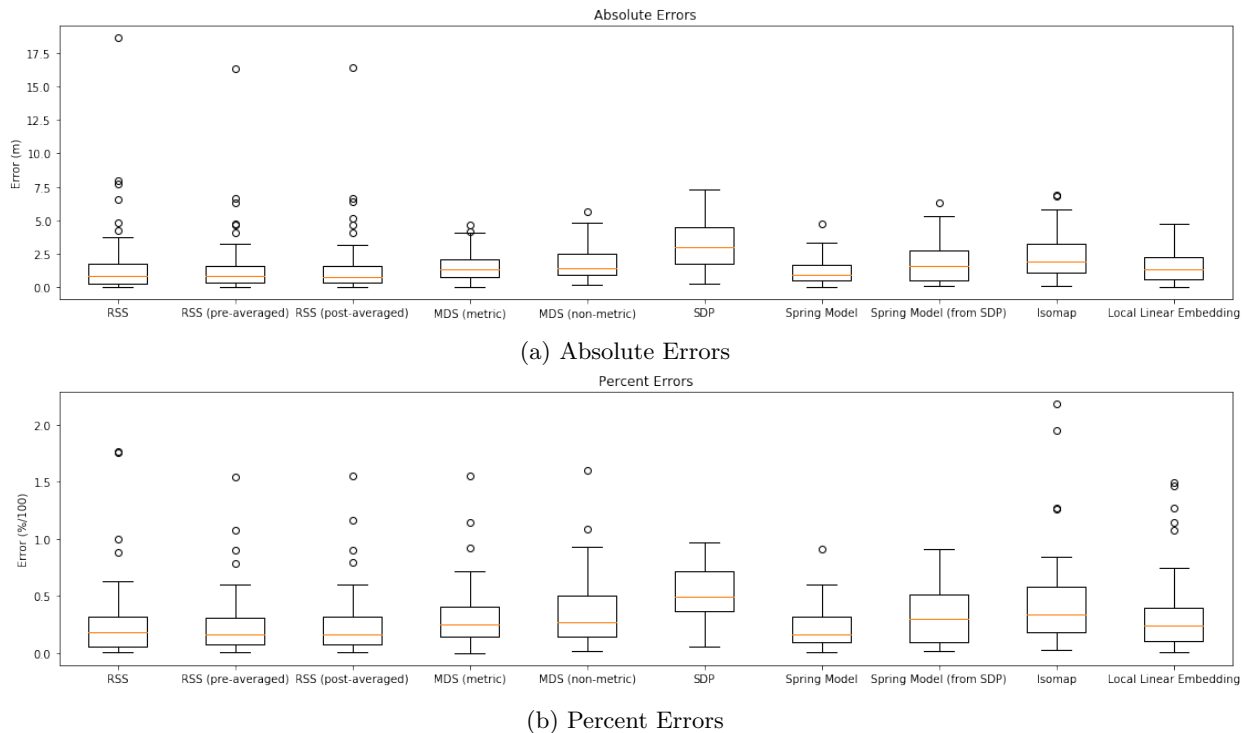


Figure 2: Errors on experimental data from 11 node network

no solution is clearly dominant, but when considering the percent error the spring model appears to just barely outperform direct estimation approaches.

Previously we have discussed performance metrics on the accuracy of the results obtained by each approach. It is important to also note discrepancies in complexity of each approach. For a network of  $n$  nodes, direct estimation requires worst-case  $O(n^2)$  computations. For MDS, the number of computations is bounded by  $O(T(n^3 + 2n^2))$  where  $T$  is the number of iterations.  $T$  is typically smaller than  $n$  and treated as a constant, so the complexity can be thought of as  $O(n^3)$ . Similarly, the complexity of the spring model is bounded by  $O(Tn^2)$  but the number of required iterations has been shown to be approximately  $n$ , simplifying to  $O(n^3)$ . Semidefinite programming when applied to network localization is on the order of  $O(n^3)$  as well. The complexity of Isomap and LLE both depend on the number of neighbors considered,  $k$ , and are bounded by  $O(2n \log(k) \log(n)) + O(n^2(k + \log(n))) + O(2n^2)$  and  $O(2n \log(k) \log(n)) + O(2nk^3) + O(2n^2)$  respectively. If low-complexity is desirable, direct estimation provides a clear advantage. However under the centralized architecture assumption, all computations can be done at the server.

The results shown in Figure 4 show the run time in seconds of each approach on the experimental data on a personal computer. Note that MDS (metric), MDS (non-metric), and the spring model were each initialized 5 times and only return the results obtained by the best initialization. Increasing the number of initialization can improve performance at the cost of computational expense.

## 5.2. Missing RSSI measurements

Previously we have noted that not all implementations can handle partial RSSI matrices. Direct estimation and the Scikit-Learn implementation of metric MDS both require estimated distances between all devices and we use a threshold RSSI value representing the noise floor of the receiver for any missing entries, making the assumption that missing RSSI values are a result of large node-node distances. This assumption may be why direct estimation and metric MDS performed well on experimental data.

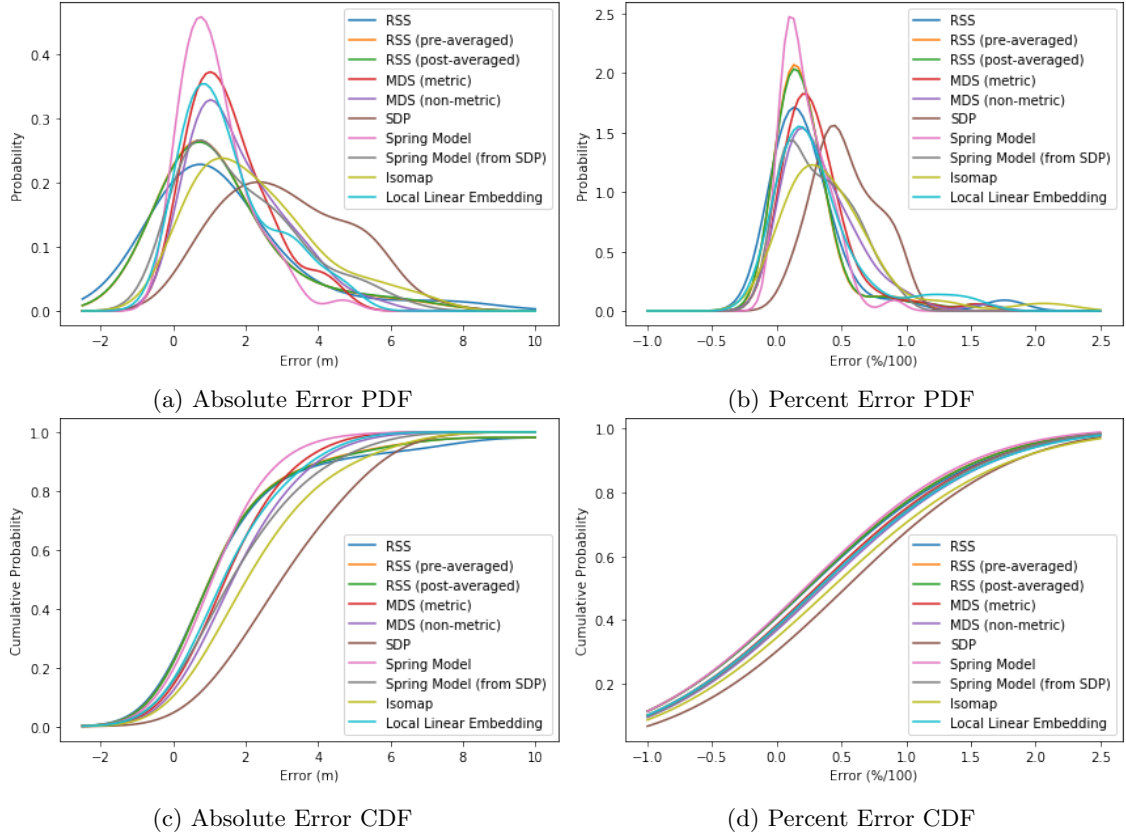


Figure 3: Error density functions

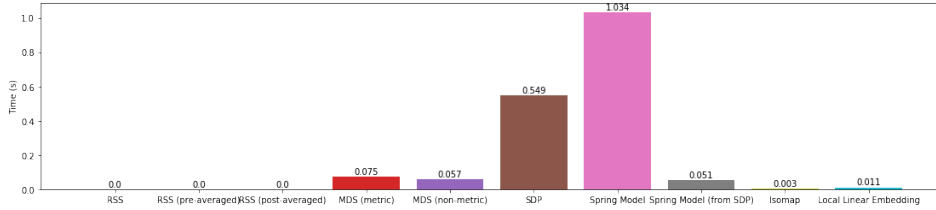


Figure 4: Run times

There is ongoing discussion of issues with iPhone-iPhone detection, relating to operating system level restrictions on background app usage [44]. Because of this, it seems reasonable to assume that while an Android-Android or iPhone-Android pair within range may record an RSSI measurement, an iPhone-iPhone pair at the same distance may not. This leads us to revisit the assumption that missed measurements are simply a result of long distances. If we assume instead that some beacon signals are dropped at random, independent of node-node distance, we observe that performance varies significantly across methods. Figure 5 shows the change in mean percent error for each approach as the number of dropped RSSI measurements increases, using the same network and measurements as Figure 2.

We see that SDP, the spring model, and the spring model initialized from SDP are the only approaches which do not see significant performance degradation when RSSI measurements are missing. Isomap, LLE, and non-metric MDS see better performance than direct estimation as well. From this we conclude that unless devices are able to guarantee measurements from all devices within Bluetooth range, network localization algorithms designed for incomplete matrices will see the best results. In fact, leveraging neighboring

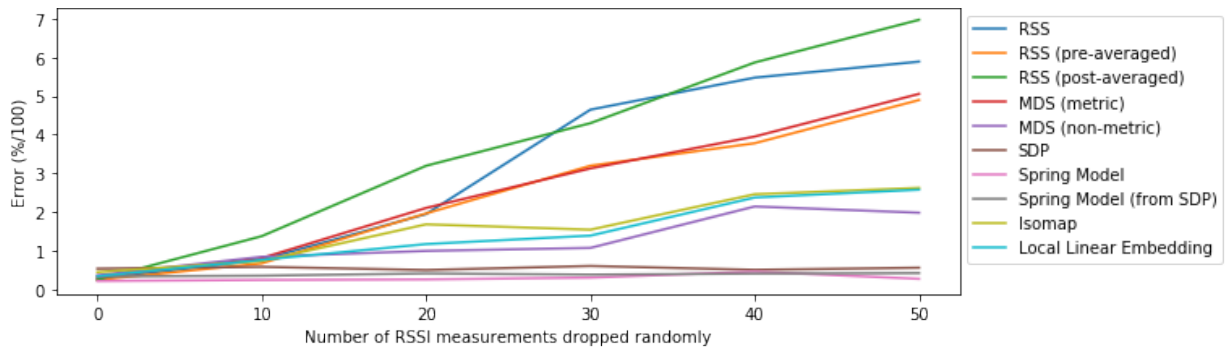


Figure 5: Incomplete RSSI matrices: Mean percent error as RSSI signals are randomly dropped

RSSI measurements through network localization may be the only option for detecting proximity between two iPhones, unless Apple eases app restrictions.

### 5.3. Common contact-logging scenarios

Figure 6 shows three common scenarios that have been previously considered when analyzing the feasibility of using BLE RSSI measurements for proximity detection [4]. The accompanying parameters fitted to data collected in these scenarios are shown in Table 2. It is immediately clear that the choice of pathloss parameters is highly dependent on the environment. This will make it challenging to design distance estimation algorithms for practical use which are generalizable enough to work indoors, outdoors, on an elevator, etc. For now, we consider each scenario and its accompanying pathloss parameters independently.

Table 2: Pathloss Parameters fitted to data from [4]

Scenario	Reference power $P_{0_{dBm}}$	Pathloss exponent $\eta$	Noise Standard Deviation $\sigma_{dB}$
Indoors	-62.919	2.316	3.441
On a train	-60.452	1.364	5.054
Outdoors	-75.014	1.7919	6.448

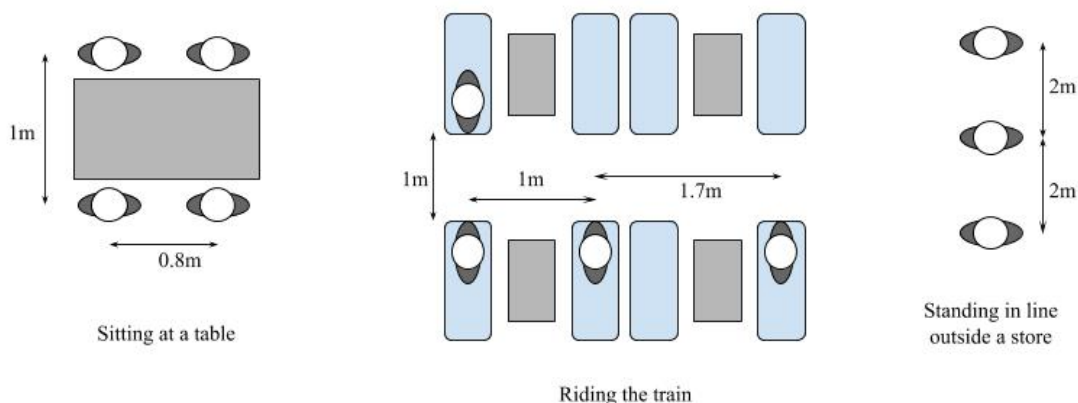


Figure 6: Common scenarios for which data was collected in [4]

Figure 7 shows the errors obtained in common scenarios for all approaches which do not require complete RSSI matrices, with direct estimation for comparison. For four people sitting around a table with their phones on the table (7a), the spring model provides the best performance. However if the four people have their phone inside their pockets (7b), SDP is the only method to find a solution where errors are at most 5x the true distance. In this case the additional attenuation caused by the physical barrier of the pocket, which is not captured in the model, renders all methods unusable.

It may be possible to use additional sensors on mobile devices like light sensors and proximity sensors to predict whether a phone is in a pocket. If obstructions can be detected, we can compensate for their presence. Figure 7c shows significant improvements in distance estimation when we assume pockets cause 20dB of attenuation [4] and their presence is detected.

For four people riding a train (Figure 7d), errors are fairly comparable although non-metric MDS, Spring Model, and Isomap see the best performance with respect to proximity detection (see Table 3). SDP and the SDP-initialized spring model both report 100% false positive rates, indicating a tendency to underestimate distances. For contact logging, high false positive rates can lead to unnecessary concern and a distrust in the technology.

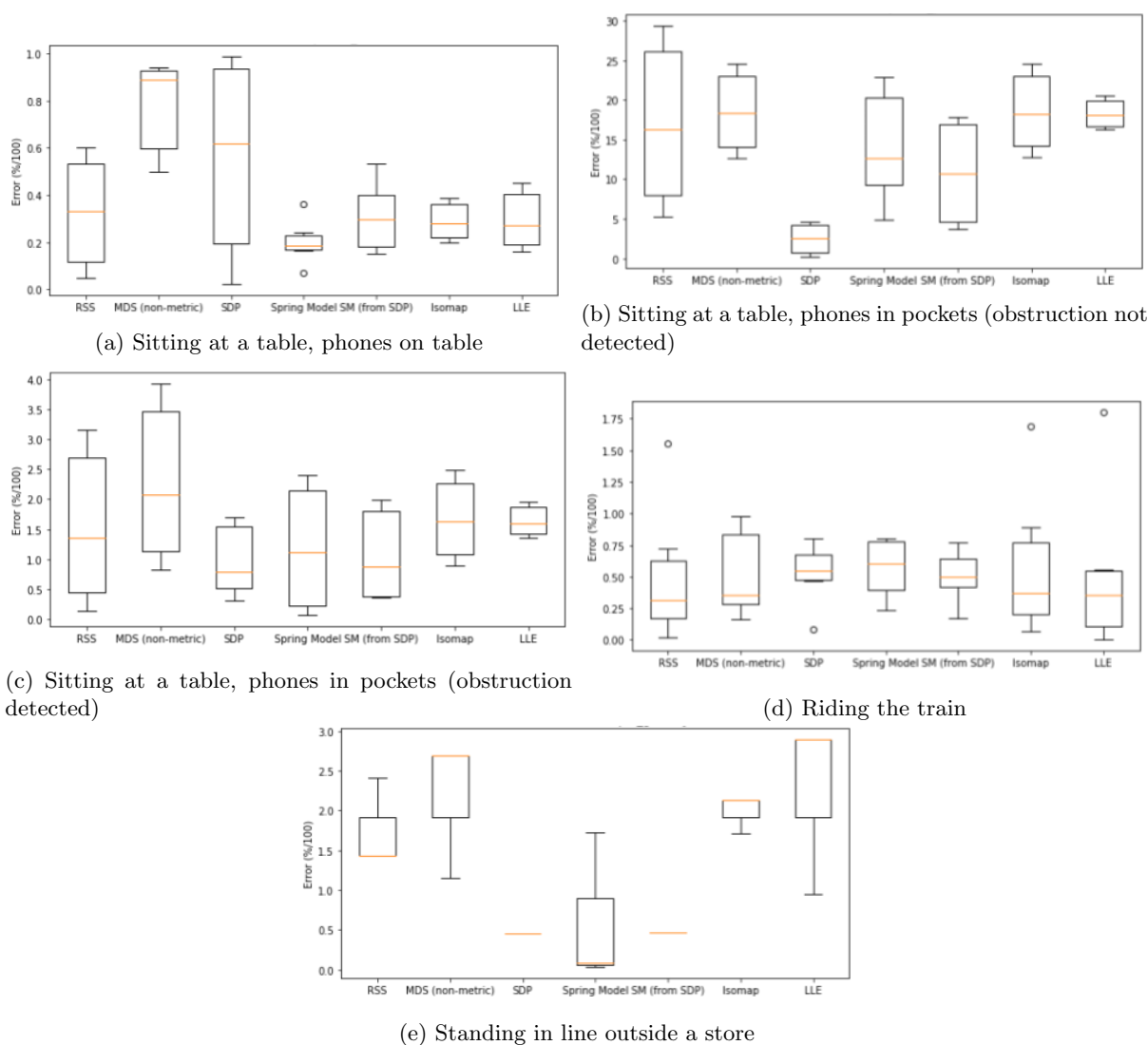


Figure 7: Percent errors in common scenarios

Table 3: Proximity detection performance in common scenarios

	Phone on table		Phone in pocket		Obstruction detected		On train		Grocery line	
	FPR	TPR	FPR	TPR	FPR	TPR	FPR	TPR	FPR	TPR
RSS	0	1	0	0	0	0.67	0.5	0.75	0	0.5
MDS (non-metric)	0	1	0	0	0	0.33	0	0.75	0	0.5
SDP	0	1	0	0.33	0	0.5	1	1	0	0.5
Spring Model	0	1	0	0	0	0.5	0	0.75	0	0.5
Spring Model (from SDP)	0	1	0	0	0	0.5	1	1	0	0.5
Isomap	0	1	0	0	0	0.33	0	0.75	0	0.5
LLE	0	1	0	0	0	0	0	0.5	0	0.5

Note that for phones in pockets, only a third of device pairs which were closer than 2 meters were detected by SDP, and none were detected by the other approaches. However when the pocket obstruction is detected and accounted for, up to two thirds of true positives were detection by direct estimation. From this we conclude that while network localization algorithms can improve inter-device distance estimation, they cannot alone overcome the fact that patterns in received signal strength depend heavily on the environment and obstructions. Automatically detecting environmental factors presents an area for future research.

## 6. Performance on Simulated Data

To test our methods on scenarios which were not already captured in available real-world datasets we developed techniques for simulating networks while attempting to preserve the noise profile seen in real-world experiments. This was used to test the viability of approaches as network size scales, how well different approaches handled varying levels of sparsity in the RSSI matrix, and the effects of different forms of real-world noise on the performance of the different distance estimation approaches. Such synthetic situations are useful as they allow for modeling of a diverse set of scenarios while having a ground-truth solution readily available. These synthetic scenarios leveraged the data captured in [4].

### 6.1. Synthetic Network Generation

We randomly generated networks of device locations and determined inter-device RSSI based upon pairwise device distance. If the distance was exactly a distance for which RSSI was measured in [4], the RSSI was randomly sampled from one of the reported RSSIs at the given distance from the data. If the distance was between two measured distances from the data, RSSI was sampled from both respective distances and linear interpolation was performed between the two measurements. If the distance was below any measured distance, RSSI was sampled from the smallest distance measured (0.5 m) as RSSI was found to change little as that distance continued to shrink. If the simulated distance was above the maximum measured distance (4 m), the devices were considered to be out of range of each other.

For all scenarios we assumed a ten percent chance that a given measurement would be missed. For all results shown, excluding Table 5, the RSSI data generated came from measurements between two Google Pixel phones in an outdoor environment.

### 6.2. Summary of Results

In Tables 4 and 5 we present the average values of our estimation approaches over a wide range of simulated network sizes and densities. Table 4 represents scenarios where measurements were sampled from Google Pixels in open air, such as in one’s hand or on a table. In comparison, Table 5 represents scenarios where measurements were sampled from varying devices in varying contexts, including in one’s pocket or purse.

As can be seen, the methods used showed substantial decrease in performance when the pathloss parameters greatly varied and were not well understood. These results indicate that a great challenge in deploying these techniques is the ability to accurately understand or control the testing environment. Investigation of

Table 4: Summarized Results for Single Device Type in Open Air

	Isomap	LLE	MDS Metric	MDS Non-Metric	RSS	RSS Post	RSS Pre	SDP	SDP + Spring	Spring Model
Avg % Error	0.50	0.50	8.10	0.50	6.60	6.60	6.60	0.50	0.40	0.30
Max % Error	10.50	10.40	103.50	26.80	307.30	307.30	307.30	3.20	3.50	11.10
TPR	0.68	0.65	0.06	0.62	0.84	0.84	0.84	0.98	0.94	0.86
FPR	0.16	0.16	0.01	0.21	0.10	0.09	0.09	0.51	0.34	0.15

Table 5: Summarized Results for Varying Device Types in Varying Context

	Isomap	LLE	MDS Metric	MDS Non-Metric	RSS	RSS Post	RSS Pre	SDP	SDP + Spring	Spring Model
Avg % Error	1.30	1.20	8.80	1.30	7.60	7.60	7.30	0.80	0.70	0.90
Max % Error	19.30	19.90	102.10	53.70	261.30	261.90	261.30	22.30	20.40	27.40
TPR	0.36	0.34	0.03	0.18	0.39	0.29	0.33	0.62	0.63	0.40
FPR	0.07	0.08	0.00	0.08	0.08	0.04	0.04	0.45	0.42	0.12

the substantial drop-off in performance showed in Table 5 indicates the change in performance is largely due to the substantial increase in attenuation seen in certain configurations. The attenuation from a pocket or purse is commonly in the range of 15 to 20 dB [4]. The major takeaway from this result is that the successful deployment of these approaches depends on being able to sense the environment and accurately predict signal attenuation across a wide range of scenarios. With that being said, we note that the spring model initialized with SDP achieves the best distance estimation performance and the best proximity detection if false negatives and false positives are equally undesirable.

### 6.3. Dense Networks

We simulated 50 scenarios where 50 devices were randomly positioned across a 100 square meter field. Figures 8 and 9 show the true positive rate (TPR) and false positive rate (FPR) achieved across the simulations. Approaches using semidefinite programming (SDP, SDP + Spring) appear to generally outperform the others in terms of TPR while also generally under-performing all others in terms of FPR, indicating they tend to return positive predictions. Direct estimation approaches (RSS, pre-averaged RSS, and post-averaged RSS) lead to high true positive rates and low false positive rates, indicating good performance with respect to proximity detection. However examining Figure 10, we see that methods which allow for missing measurements greatly outperform the direct approaches with respect to distance estimation. The spring model, Isomap, and LLE appear well-suited for both proximity detection and distance estimation.

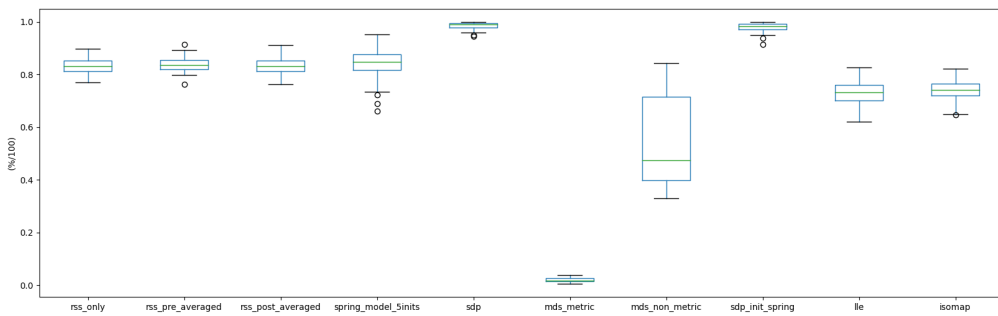


Figure 8: True Positive Rates for 50 devices in 100 square meters

### 6.4. Sparse Networks

The previous simulated data resulted in dense network graphs. We are also interested in performance in sparse networks where devices are spread across large areas therefore RSSI measurements are not available for many device pairs. We simulate 50 devices randomly positioned across a 400 square meter field. We

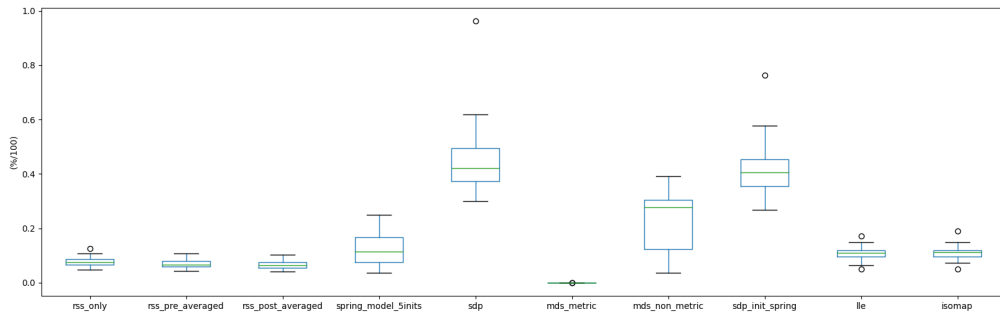


Figure 9: False Positive Rates for 50 devices in 100 square meters

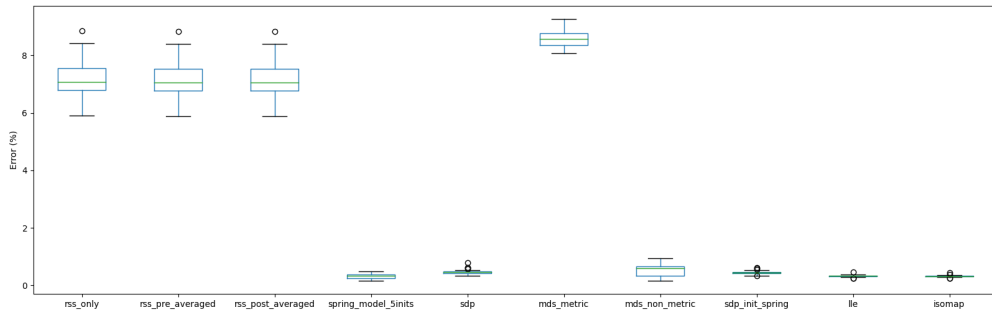


Figure 10: Mean Percent Error for 50 devices in 100 square meters

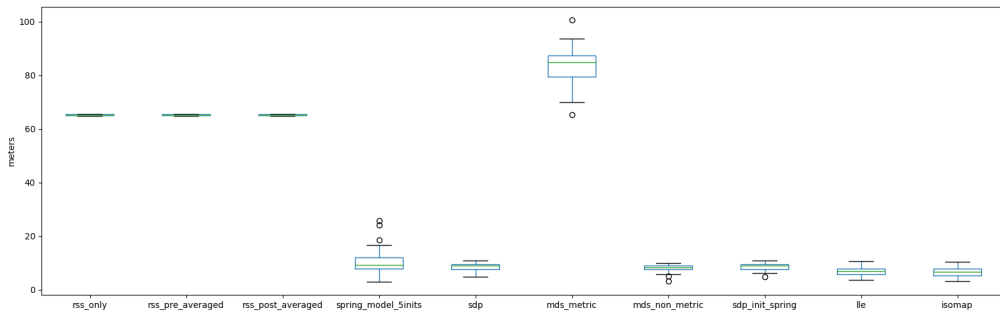


Figure 11: Maximum Error for 50 devices in 100 square meters

observe similar patterns, with SDP-based methods leading to the most true positives but also the most false positives, and direct methods leading to good proximity detection accuracy but poor distance estimate accuracy. These results are omitted for brevity.

### 6.5. Large Networks

We are also interested in examining how these approaches scale to larger networks. For this we simulate 100 nodes over a 400 square meter field. For these large simulated networks (Figure 12), the proximity detection and distance estimation results agree with those obtained in Sections 6.3 and 6.4. As discussed in

section 5, runtimes increased across all methods as the number of nodes grew. We noted that the open-source optimized implementations of network localization algorithms saw average runtimes of 2-5 seconds for 100 node networks on our hardware, likely acceptable for most use cases. However if scalably fast calculations are the main priority, the averaged direct estimation approaches are the best choice.

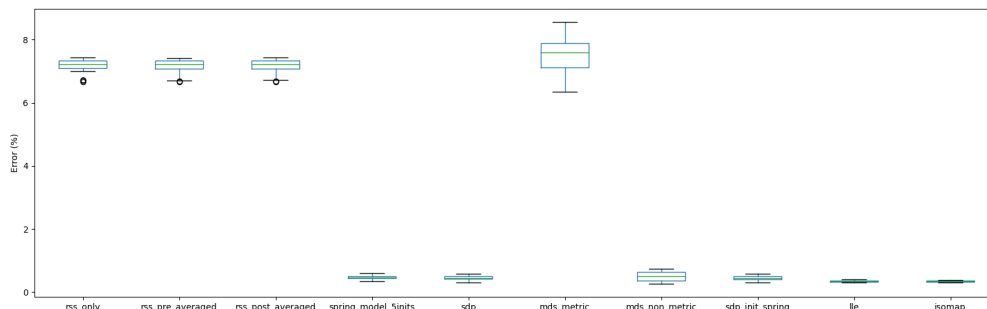


Figure 12: Mean Percent Error for 100 nodes in 400 square meters

## 7. Conclusions and Future Work

In this work we have surveyed several approaches to estimating inter-device distances using network localization algorithms to explore the emerging application of automated contact logging. We have found that the choice of algorithm is quite nuanced, and the success of algorithms is largely dependent on how representative the pathloss model is of the actual environment. Our experiments indicate that in ideal settings when all RSSI measurements are available, direct estimation provides the best proximity detection and lowest complexity while the spring model narrowly outperforms direct approaches with respect to inter-device distance estimation. Under more realistic assumptions, SDP sees good distance estimate accuracy and is the most likely to identify all true positives (distances less than 2 meters), but it is also the most likely to lead to false positives. The spring model again sees the best distance estimation and good proximity detection, but there is some variance in performance as the result depends on a random initialization.

Importantly, we have also observed that context (i.e. indoors, outdoors, in a pocket, etc) has a greater effect on the resulting distance estimate matrix than the network localization approach. Similarly, the relationship between distance and signal strength is not the same for all devices. The OpenTrace Community has provided access to the RSSI measurements which correspond to 2 meters for 18 phone models in Figure 13 [3]. With the increasing availability of this data, we can specialize our RSSI-to-distance model based on device type. We have shown that the ability to gauge context via data from ambient light sensors and/or proximity sensors to detect obstructions would increase performance across all approaches.

All of the methods presented in this work are anchorless, “one-shot” localization approaches, meaning we assume no locations are known in advance, all measurements are taken at one time, and no data is available before or after this moment. Further improvements could be made taking into account the location of cell phone towers or other potential beacons, or by leveraging time sequences of measurements and user mobility models.

As accurately estimating distance from Bluetooth measurements is a challenging and timely problem, we intend to continue research on improving these models and algorithms. We are working closely with the Covid Community Alert team, and plan on incorporating the findings from this work in their open-source anonymous protocol.



Chamber Testing of Signal Strength at 2 metres

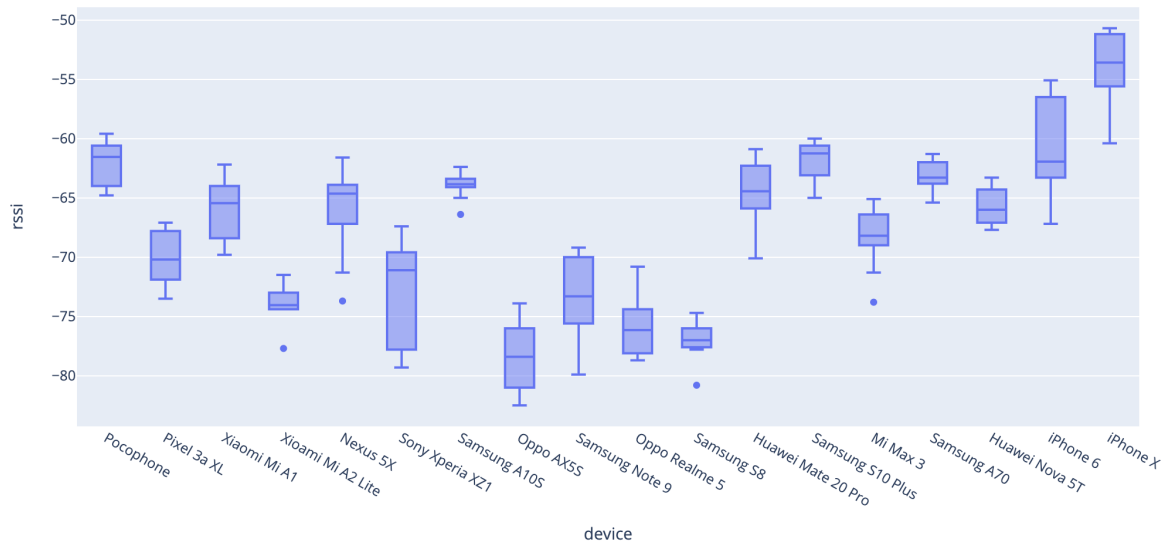


Figure 13: RSSI data for devices at 2 meters available from <https://github.com/opentrace-community> [3]

## References

- [1] Covid community alert: World-level open-source anonymous protocol, <https://coronavirus-outbreak-control.github.io/web/> (2020).
- [2] Pact: Private automated contact tracing, <https://pact.mit.edu/> (2020).
- [3] J. Bay, J. Kek, A. Tan, C. S. Hau, L. Yongquan, J. Tan, T. A. Quy, Bluetrace: A privacy-preserving protocol for community-driven contact tracing across borders, Government Technology Agency-Singapore, Tech. Rep (2020).
- [4] D. J. Leith, S. Farrell, Coronavirus contact tracing: Evaluating the potential of using bluetooth received signal strength for proximity detection (2020).
- [5] S. Liu, Y. Jiang, A. Striegel, Face-to-face proximity estimation using bluetooth on smartphones, *IEEE Transactions on Mobile Computing* 13 (4) (2014) 811–823.
- [6] Wireless range estimation, <https://github.com/ANRGUSC/WirelessRangeEstimation> (2020).
- [7] H. Cai, V. W. Zheng, K. Chang, A comprehensive survey of graph embedding: Problems, techniques, and applications, *IEEE Transactions on Knowledge and Data Engineering* 30 (09) (2018) 1616–1637. doi:10.1109/TKDE.2018.2807452.
- [8] J. Bachrach, C. Taylor, Localization in sensor networks, *Handbook of sensor networks: Algorithms and Architectures* 1 (2005) 277–289.
- [9] A. J. Izenman, Introduction to manifold learning, *Wiley Interdisciplinary Reviews: Computational Statistics* 4 (5) (2012) 439–446.
- [10] F. Young, Multidimensional scaling, *encyclopedia of statistical sciences (volume 5)*, kotz-johnson, ed (1985).
- [11] Distance, similarity, and multidimensional scaling, <https://pages.mtu.edu/~shanem/psy5220/daily/Day16/MDS.html> (Mar. 2019).
- [12] Manifold learning, <https://scikit-learn.org/stable/modules/manifold.html> (2019).
- [13] W. S. Torgerson, Multidimensional scaling: I. theory and method, *Psychometrika* 17 (4) (1952) 401–419.
- [14] Y. Shang, W. Rumi, Y. Zhang, M. Fromherz, Localization from connectivity in sensor networks, *IEEE Transactions on parallel and distributed systems* 15 (11) (2004) 961–974.
- [15] Y. Shang, W. Ruml, Improved mds-based localization, in: *IEEE INFOCOM 2004*, Vol. 4, IEEE, 2004, pp. 2640–2651.
- [16] J. De Leeuw, Applications of convex analysis to multidimensional scaling (2005).
- [17] C. Savarese, J. M. Rabaey, J. Beutel, Location in distributed ad-hoc wireless sensor networks, in: *2001 IEEE international conference on acoustics, speech, and signal processing. proceedings (Cat. No. 01CH37221)*, Vol. 4, IEEE, 2001, pp. 2037–2040.
- [18] N. B. Priyantha, H. Balakrishnan, E. Demaine, S. Teller, Anchor-free distributed localization in sensor networks, in: *Proceedings of the 1st international conference on Embedded networked sensor systems*, 2003, pp. 340–341.
- [19] P. Biswas, T. C. Lian, T. C. Wang, Y. Ye, Semidefinite programming based algorithms for sensor network localization, *ACM Transactions on Sensor Networks* 2 (2) (2006) 188–220. doi:10.1145/1149283.1149286.
- [20] L. Doherty, L. El Ghaoui, et al., Convex position estimation in wireless sensor networks, in: *Proceedings IEEE INFOCOM 2001. Conference on Computer Communications. Twentieth Annual Joint Conference of the IEEE Computer and Communications Society (Cat. No. 01CH37213)*, Vol. 3, IEEE, 2001, pp. 1655–1663.

- [21] G. Mao, B. Fidan, B. D. Anderson, Wireless sensor network localization techniques, *Computer networks* 51 (10) (2007) 2529–2553.
- [22] J. Wang, R. K. Ghosh, S. K. Das, A survey on sensor localization, *Journal of Control Theory and Applications* 8 (1) (2010) 2–11.
- [23] T. J. Chowdhury, C. Elkin, V. Devabhaktuni, D. B. Rawat, J. Oluoch, Advances on localization techniques for wireless sensor networks: A survey, *Computer Networks* 110 (2016) 284–305.
- [24] K. Langendoen, N. Reijers, Distributed localization in wireless sensor networks: a quantitative comparison, *Computer networks* 43 (4) (2003) 499–518.
- [25] L. Yang, R. Jin, Distance metric learning: A comprehensive survey, *Michigan State University* 2 (2) (2006) 4.
- [26] N. Saeed, H. Nam, M. I. U. Haq, D. B. Muhammad Saqib, A survey on multidimensional scaling, *ACM Computing Surveys (CSUR)* 51 (3) (2018) 1–25.
- [27] L. Van Der Maaten, E. Postma, J. Van den Herik, Dimensionality reduction: a comparative, *J Mach Learn Res* 10 (66-71) (2009) 13.
- [28] N. Patwari, A. O. Hero, Manifold learning algorithms for localization in wireless sensor networks, in: 2004 IEEE international conference on acoustics, speech, and signal processing, Vol. 3, IEEE, 2004, pp. iii–857.
- [29] J. Kashniyal, S. Verma, K. P. Singh, Wireless sensor networks localization using progressive isomap, *Wireless Personal Communications* 92 (3) (2017) 1281–1302.
- [30] D. J. Leith, S. Farrell, Measurement-based evaluation of google/apple exposure notification api for proximity detection in a commuter bus, *arXiv preprint arXiv:2006.08543* (2020).
- [31] H. Cho, D. Ippolito, Y. W. Yu, Contact tracing mobile apps for covid-19: Privacy considerations and related trade-offs, *arXiv preprint arXiv:2003.11511* (2020).
- [32] J. Li, X. Guo, Covid-19 contact-tracing apps: A survey on the global deployment and challenges, *arXiv preprint arXiv:2005.03599* (2020).
- [33] S. Diamond, S. Boyd, CVXPY: A Python-embedded modeling language for convex optimization, *Journal of Machine Learning Research* 17 (83) (2016) 1–5.
- [34] A. Agrawal, R. Verschueren, S. Diamond, S. Boyd, A rewriting system for convex optimization problems, *Journal of Control and Decision* 5 (1) (2018) 42–60.
- [35] B. O’Donoghue, E. Chu, N. Parikh, S. Boyd, Conic optimization via operator splitting and homogeneous self-dual embedding, *Journal of Optimization Theory and Applications* 169 (3) (2016) 1042–1068.  
URL <http://stanford.edu/~boyd/papers/scs.html>
- [36] B. O’Donoghue, E. Chu, N. Parikh, S. Boyd, SCS: Splitting conic solver, version 2.1.2, <https://github.com/cvxgrp/scs> (Nov. 2019).
- [37] P. Biswas, T. C. Liang, K. C. Toh, Y. Ye, T. C. Wang, Semidefinite programming approaches for sensor network localization with noisy distance measurements, *IEEE Transactions on Automation Science and Engineering* 3 (4) (2006) 360–371. doi:10.1109/TASE.2006.877401.
- [38] A. Beck, P. Stoica, J. Li, Exact and approximate solutions of source localization problems, *IEEE Transactions on Signal Processing* 56 (5) (2008) 1770–1778. doi:10.1109/TSP.2007.909342.
- [39] L. Guttman, A general nonmetric technique for finding the smallest coordinate space for a configuration of points, *Psychometrika* 33 (4) (1968) 469–506.
- [40] J. De Leeuw, P. Mair, Multidimensional scaling using majorization: Smacof in r (2011).
- [41] J. B. Tenenbaum, V. De Silva, J. C. Langford, A global geometric framework for nonlinear dimensionality reduction, *science* 290 (5500) (2000) 2319–2323.
- [42] S. T. Roweis, L. K. Saul, Nonlinear dimensionality reduction by locally linear embedding, *science* 290 (5500) (2000) 2323–2326.
- [43] K. Yedavalli, B. Krishnamachari, S. Ravula, B. Srinivasan, Ecolocation: a sequence based technique for rf localization in wireless sensor networks, in: *IPSN 2005. Fourth International Symposium on Information Processing in Sensor Networks, 2005.*, IEEE, 2005, pp. 285–292.
- [44] J. O’Halloran, iPhone issues see uk government dump centralised model for covid-19 contact-tracing app, <https://www.computerweekly.com> (Jun 2020).